

Received October 23, 2020, accepted October 29, 2020, date of publication November 4, 2020, date of current version November 17, 2020.

Digital Object Identifier 10.1109/ACCESS.2020.3035896

Neural Network Predictive Control of Swing Phase for a Variable-Damping Knee Prosthesis With Novel Hydraulic Valve

XIAOMING WANG^{ID}, (Member, IEEE), QIAOLING MENG^{ID}, (Member, IEEE),
HE LAN, (Member, IEEE), ZHANG ZHEWEN, (Member, IEEE),
CHANGLONG CHEN, (Member, IEEE), AND HONGLIU YU^{ID}, (Member, IEEE)

Rehabilitation Engineering and Technology Institute, University of Shanghai for Science and Technology, Shanghai 200093, China

Shanghai Engineering Research Center of Assistive Devices, Shanghai 200093, China

Key Laboratory of Neural-Functional Information and Rehabilitation Engineering of the Ministry of Civil Affairs, Shanghai 200093, China

Corresponding author: Hongliu Yu (yhl98@hotmail.com)

This work was supported in part by the National Key Research and Development Program of China under Grant 2018YFB1307303, and in part by the National Natural Science Foundation of China under Grant 62073224.

ABSTRACT It is necessary to develop an effective knee prosthesis to recover the lost mobility of amputees. Variable-damping knee prostheses utilizing hydraulic dampers offer several advantages, but current researches are limited in approaching healthy knee behavior. To improve the gait symmetry, this study proposed a variable-damping knee prosthesis with a novel hydraulic damper using neural network predictive control (NNPC) scheme during swing phase. The external fan valve structure of the hydraulic damper can not only realize independent and continuous adjustment of flexion and extension damping by a single motor, but also can effectively avoid the damping adjustment failure caused by excessive load. NNPC was proposed as a controller to control the novel hydraulic damper during swing phase. The online simulation is carried out based on MATLAB utilizing the workbench composed of knee prosthesis prototype and self-built gait simulation and evaluation platform, so as to preliminarily verify the online feasibility and effectiveness of the algorithm at different speeds. The offline gait symmetry experiments are designed to more intuitively and effectively compare the performance of NNPC with the fuzzy logical control proposed in previous work. The results show that NNPC improves the gait symmetry from the fuzzy logical control at different walking speeds as the values of symmetry indices are significantly decrease in the range of 5.13% to 33.96%. These results indicate that the proposed variable-damping knee prosthesis can make a good performance on improving the approximation of healthy gait characteristics and meet the fundamental requirements of walking at various walking speeds.

INDEX TERMS Variable-damping knee prosthesis, hydraulic damper, neural network predictive control (NNPC), gait symmetry.

I. INTRODUCTION

Every year, thousands of people all over the world lose their lower limbs because of vascular diseases, traumata, and tumors [1]. It is necessary to develop an effective prosthesis to recover the lost mobility of amputees and assist them to participate in daily activities. With recent advances in computer and sensor technologies in the last few decades, the use of robots for various applications has increased enormously [2], [3], and a technological revolution in the prosthetic industry

The associate editor coordinating the review of this manuscript and approving it for publication was Jonghoon Kim^{ID}.

has taken place. The knee prosthesis is one of the most important part of lower limb prosthesis, which can be classified into three types: mechanically passive, variable-damping, and powered knee prostheses [4]. The mechanically passive knee prosthesis can operate without power supply, but it can only generate knee damping for one constant walking speed. The variable-damping knee prosthesis is superior to the passive knee in terms of energy consumption, stability, adaptability to environmental changes, and ability to respond to walking speed [5], [8]. Powered knee prostheses have mechanisms that generate positive energy and damping forces, enabling amputees to perform more complex activities, such

as standing up from a sitting position and walking up stairs [9], [10]. However, this kind of knee prosthesis requires a large actuator and consumes a high level of energy, resulting in increased weight and reduced battery life [11]. To sum up, variable-damping knee prosthesis is still the mainstream of current research, as the proportion of the knee joint acting as a damper is much higher than that of the actuator in the normal walking process.

A gait cycle contains a stance phase and a swing phase. The stance phase aims to provide sufficient damping force to ensure the stability of the gait, without requiring high adaptability to different walking speeds. The swing phase aims to ensure the flexibility of the gait, which requires a rapid response to the changes in walking speed and environment [12]. Hydraulic damper, which can satisfy both the stability of stance phase and the flexibility of swing phase, is widely used in variable-damping knees [13]. Hydraulic variable-damping knee prostheses are nonlinear and strong coupling underactuated systems, so it is very important but difficult to control the prostheses to track the planned gait trajectory. Cao *et al.* [14], [15] of our team proposed a fuzzy logical speed adaptive control scheme based on maximum flexion angle during swing phase to realize the automatic adjustment of damping, but the walking speed need be classified and a knowledge base containing the mapping relationship between the walking speed and the valve opening need be established, which led to the limitation of speed adaptive. Preitl *et al.* [16] presented PI-fuzzy controllers based on Iterative Feedback Tuning (IFT) and the Iterative Learning Control (ILC), which, like the research of Cao *et al.* [14], [15], also had the same limitation of establishing an offline knowledge base when applied to control knee prosthesis. Chen and Sun [17] proposed a new control strategy for a class of underactuated systems that can treat the various constraints including actuated and unactuated state constraints and the constraints on some specific composite variables. The good performance of this method was verified by applying it to two examples where the constraint is invariant when the target location is determined. The proposed method may not be suitable for controlling the trajectory of the knee prosthesis, because the state constraint during walking is equivalent to the contralateral knee trajectory, which will change with the change of walking speed, road conditions and other uncertainties. Seid *et al.* [18] designed a variable-damping controller for a single-axis knee prosthesis with hydraulic damper during swing phase. However, the controller did not perform well in terms of ground clearance because it caused the prosthetic knee angle to be significantly different from the healthy angle. Richter *et al.* [19] developed a virtual controller for a variable-damping knee prosthesis that can determine the valve positions to make the actual torque approximate to the healthy knee torque. Although the simulation results indicated that the controller can realize angular trajectory tracking, the specific valve structure was not proposed, and the simulation was only carried out on the basis of conceptual design. For variable-damping knee prostheses,

the gait symmetry depends mainly on the accuracy of the damping control of swing phase. Therefore, it is of great significance to design a valve structure that is easy to adjust and a speed adaptive control strategy that can realize accurate angle tracking during swing phase.

This research proposes a novel valve structure for variable-damping knee prosthesis, which can continuously adjust the flexion and extension damping by a single motor, and proposes a control strategy using neural network predictive control (NNPC) during swing phase based on the proposed valve structure, with the ability to predict future knee angle and adapt to different walking speeds [20]. Compared with the traditional optimal control, which requires global optimization to realize the calculation of feedback control, the proposed neural network predictive control method has two main features, namely local rolling optimization and predictive ability, so it can realize real-time control with less calculation and can generate optimal damping forces in advance to compensate for errors due to hydraulic damper response time, model uncertainty, and external interference. In this article, a coupling modeling of knee prosthesis consist of a double pendulum dynamics model, and a hydraulic damping numerical model was established. The simulation was carried out based on MATLAB platform utilizing the coupling model of workbench composed of knee prosthesis prototype and self-built gait simulation and evaluation platform, so as to preliminarily verify the online feasibility and effectiveness of the algorithm at different speeds. The offline gait symmetry experiments were designed to more intuitively and effectively compare the performance of NNPC with the fuzzy logical control proposed in previous work [14]. The main contributions of this article are as follows.

- 1) This article first applies predictive control to the damping control of hydraulic knee prosthesis, and its good performance on improving the approximation of healthy gait characteristics at various walking speeds is proven by gait symmetry experiments.
- 2) The novel external fan valve structure of the hydraulic damper can not only realize independent and continuous adjustment of flexion and extension damping by a single motor, but also can effectively avoid the axial load acting on the motor in the damping cylinder.
- 3) The proposed control method can be extended to solve the control problem of a class of nonlinear and strong coupling underactuated systems that need to generate optimal control variables in advance to compensate for errors due to actuators response time, model uncertainty, and external interference.

II. PROSTHESIS DESIGN AND SWING PHASE COUPLING MODELING

A. DYNAMIC MODEL OF DOUBLE PENDULUM COUPLED WITH HYDRAULIC DAMPER

The connection between ankle, foot and leg tube of the lower limb prosthesis system can be equivalent to rigidity

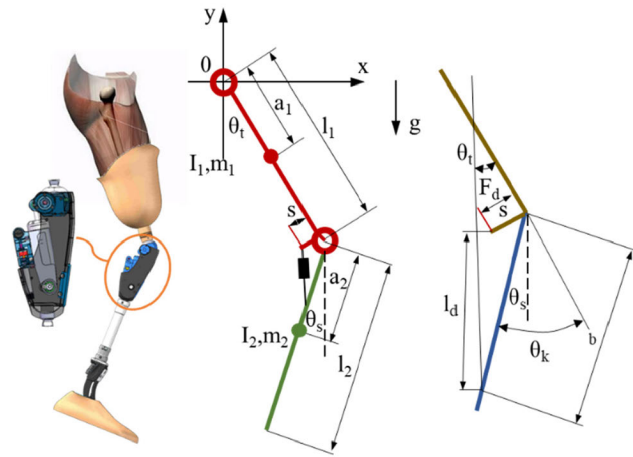


FIGURE 1. Dynamic model of double pendulum coupled with hydraulic damper.

connection, so the system can be simplified as a double pendulum dynamics model, which represents the motion of thigh and calf in the sagittal plane respectively [18]. When assembling the actual prosthetic model, static and dynamic alignment should be carried out first to make the gravity line on the prosthetic side coincide with the gravity line on the healthy side, so as to minimize the error between the desired torque and the actual torque. Therefore, the deviation in the position of the center of gravity caused by the simplified model can be ignored. The double pendulum dynamics model coupled with the hydraulic damper used to simulate swing phase of knee prosthesis is shown in Fig. 1. The specifications and values of the parameters are shown in Table 1, where median percentiles of anthropometry dimensions of Chinese male adults are obtained based on the Chinese National Standard of China GB/T 10000-1988 [21].

Assuming that there is no friction force, the double pendulum dynamics model can be expressed as below by using Lagrange formula [18].

$$D(\theta)\ddot{\theta} + C(\theta, \dot{\theta})\dot{\theta} + G(\theta) = \Gamma \quad (1)$$

The inertial matrix $D(\theta)$ can be expressed as

$$D(\theta) = \begin{bmatrix} m_1 a_1^2 + I_1 + m_2 l_1^2 & -m_2 l_1 a_2 \cos(\theta_t + \theta_s) \\ -m_2 l_1 a_2 \cos(\theta_t + \theta_s) & m_2 a_2^2 + I_2 \end{bmatrix} \quad (2)$$

The Coriolis and centrifugal terms $C(\theta, \dot{\theta})$ can be expressed as

$$C(\theta, \dot{\theta}) = \begin{bmatrix} m_2 l_1 a_2 (\dot{\theta}_s)^2 \sin(\theta_t + \theta_s) \\ m_2 l_1 a_2 (\dot{\theta}_t)^2 \sin(\theta_t + \theta_s) \end{bmatrix} \quad (3)$$

The gravity vector $G(\theta)$ can be expressed as.

$$G(\theta) = \begin{bmatrix} m_1 g a_1 \sin(\theta_t) + m_2 g l_1 \sin(\theta_t) \\ m_2 g a_2 \sin(\theta_s) \end{bmatrix} \quad (4)$$

TABLE 1. Parameters of the double pendulum dynamics model.

Parameters	Specification	Value
m_1	Thigh mass	9.900 kg
m_2	Shank mass	2.600 kg
a_1	Distance of the thigh mass center from the hip joint	0.267 m
a_2	Distance of the shank mass center from the knee joint	0.176 m
I_1	Thigh moment of inertia	0.031 kgm ²
I_2	Shank moment of inertia	0.032 kgm ²
l_1	Thigh length	0.550 m
l_2	Shank length	0.400 m
s	Offset between the knee center and location of attachment of damper piston on the thigh	0.016 m
b	Distance between the knee center and location of the damper attachment on the shank	0.128 m
θ_t	Absolute angle of thigh from the horizontal	variable
θ_s	Absolute angle of shank from the vertical	variable
θ_k	Knee angle	variable
l_d	Length of the damper	variable
T_1	Hip torque	variable

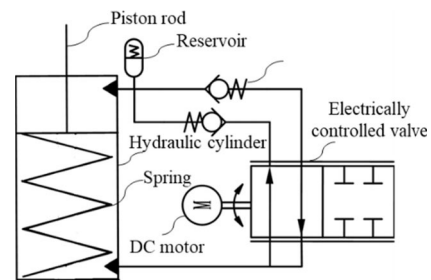


FIGURE 2. The schematic diagram of the hydraulic damping system.

The hip and knee input parameter matrices matrix Γ can be expressed as

$$\Gamma = \begin{bmatrix} T_1 + F_d a \sin(\theta_s - \beta) \\ -F_d a \sin(\theta_s - \beta) \end{bmatrix} \quad (5)$$

The thigh and calf angle vector matrix θ can be expressed as

$$\theta = \begin{bmatrix} \theta_t \\ \theta_s \end{bmatrix} \quad (6)$$

The torque generated at the knee joint during swing phase can be calculated by

$$\begin{aligned} \tau_k = & m_2 a_2^2 \ddot{\theta}_s - m_2 l_1 a_2 \ddot{\theta}_t \cos(\theta_t + \theta_s) \\ & + m_2 l_1 a_2 (\dot{\theta}_t)^2 \sin(\theta_t + \theta_s) \\ & + I_2 \ddot{\theta}_s + m_2 g a_2 \sin(\theta_s) \end{aligned} \quad (7)$$

B. NOVEL VALVE STRUCTURE DESIGN AND HYDRAULIC DAMPING NUMERICAL MODEL

The aim of the hydraulic damper used in the knee prosthesis is to provide a good approximation of the behavior of a

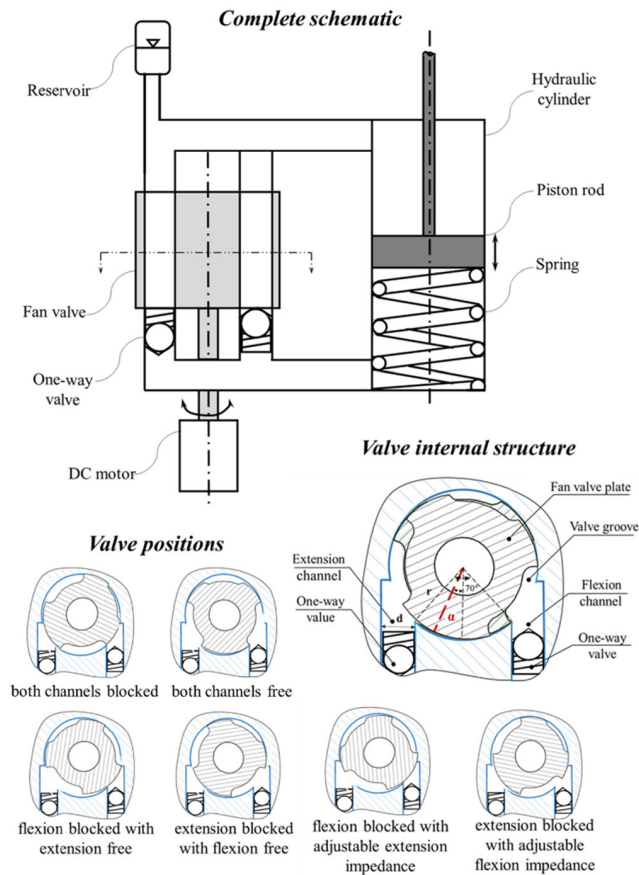


FIGURE 3. Principle and internal structure of the novel valve.

healthy knee, by supplying the same torque characteristic as a healthy knee joint during swing phase [22]. As shown in Fig. 2, a spring is arranged in the hydraulic cylinder. When the knee flexes, the piston rod moves downward, and the spring compresses and stores energy. When the knee extends, the spring releases energy. The upper and lower ends of the hydraulic cylinder respectively lead out two hydraulic oil channels with one-way valve in different directions, forming a flexion hydraulic oil circuit and an extension hydraulic oil circuit. An electrically controlled valve can simultaneously adjust the hydraulic oil flow in both circuits, so as to adjust the flexion and extension damping torque dynamically.

As shown in Fig. 3, the two oil channels mentioned above coincide with two valve grooves of the fan valve respectively two notches on the valve respectively. The fan valve rotates continuously to adjust the overlap area between the valve grooves and hydraulic oil channels. Varying the valve angle between the primary positions adjusts the impedance to flow.

The hydraulic damper is a spring/damper system. Damping torque (τ_{kd}) of the hydraulic damper at knee prosthesis can be obtained as

$$\tau_{kd} = (F_d + k \Delta x) L \quad (8)$$

where F_d is the resistance of the hydraulic cylinder, k is the elastic constant of the compression spring, Δx is the

displacement of the piston rod, and L is the length of the effective moment arm which can be obtained as

$$L = \frac{bs \cos(\theta_s - \theta_t)}{\sqrt{b^2 + s^2 + 2bs \sin(\theta_s - \theta_t)}} \quad (9)$$

The resistance of the hydraulic cylinder can be represented as

$$F_d = \Delta P A \quad (10)$$

where A is an effective flow area of the cylinder and ΔP is the pressure of the cylinder which can be represented as

$$\Delta P = \frac{\rho A^2 V^2}{2C_d^2 A_0^2} \quad (11)$$

where V is the speed of the piston rod, A_0 is the flow area of the fan valve channel, C_d is the flow coefficient of the valve and ρ is the density of hydraulic oil.

The length of the damper l_d is a variable during the motion which can be expressed as

$$l_d = \sqrt{b^2 + s^2 + 2bs \cdot \sin(\theta_s - \theta_t)} \quad (12)$$

so the speed of the damper piston V can be expressed as

$$V = \dot{l}_d = \frac{bs \cdot \cos(\theta_s - \theta_t) (\dot{\theta}_s - \dot{\theta}_t)}{\sqrt{b^2 + s^2 + 2bs \cdot \sin(\theta_s - \theta_t)}} \quad (13)$$

The flow area of the fan valve channel A_0 can be determined by

$$A_0 = 2 \int_{r[\cos(55^\circ - \alpha) - \sin 35^\circ]}^d \sqrt{\left(\frac{d}{2}\right)^2 - t^2} dt \quad (14)$$

where $\alpha \in [-35^\circ, 35^\circ]$ is the rotation angle of fan valve, r is the radius of fan valve and d is the diameter of the extension and flexion channels.

In this article, $r = 5$ mm, $d = 2.50$ mm, $\rho = 870$ kg/m³, $A = 5.37 \times 10^{-4}$ m², $C_d = 0.7$, $k = 1.4 \times 10^3$ N/m.

From (8) and (14), the torque at knee can be written as (15), as shown at the bottom of the next page.

Equation (15) shows the relationship between the torque at knee and the valve rotation angle can be obtained by measuring the hip angle and knee angle when the structure parameters of knee prosthesis and human parameters are given [23].

C. SIMULATION OF SWING PHASE COUPLING MODEL

Ideally, the DC motor controls the rotation of the fan valve in real time to provide the same damping torque as the healthy knee, which can be expressed as

$$\tau_{kd} = \tau_k \quad (16)$$

The desired knee angle data ($\theta_k(\text{desired})$) and absolute angle of thigh from the horizontal (θ_t) and the desired trajectory of the limb end were measured by a gait and motion evaluation system (Noraxon MR3, Noraxon CO., LTD., USA) at slow speed of 0.6m/s, medium speed of 1.1m/s and fast speed of 1.6m/s. The subject walked on a treadmill at each of the three

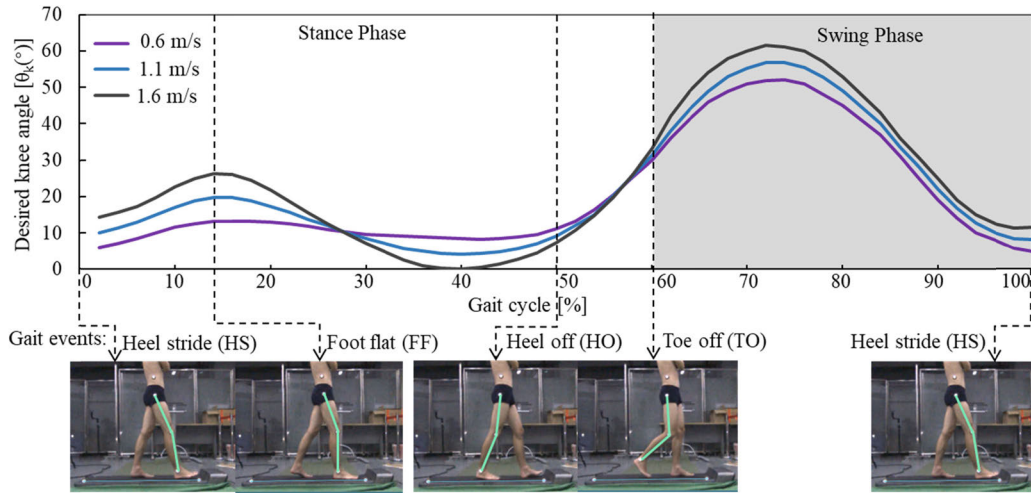


FIGURE 4. Desired knee angle of one gait cycle at different speeds.

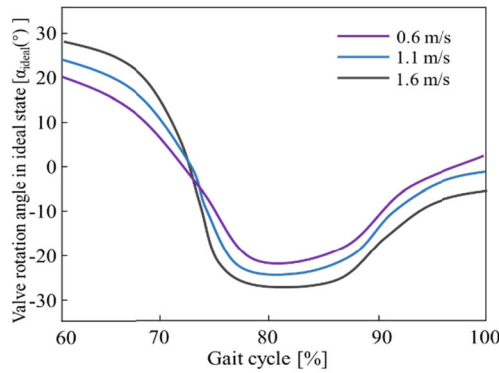


FIGURE 5. The valve rotation angle in ideal state during swing phase at different speeds.

specific speeds. Four marks were pasted on the waist, hip, knee and ankle joints of the subject, and two markers were pasted on the edge of the treadmill to serve as a benchmark. A high-speed camera with a resolution of 1920×1080 pixels and capable of recording 150 frames per second was used to record lower limb movements and to obtain kinematic data by averaging 50 consecutive gait cycles. Fig. 4 shows the example of desired knee angle data ($\theta_k^{(desired)}$) of three walking speeds and raw images that were captured from the system.

The valve rotation angle in ideal state during swing phase (α_{ideal}) were calculated in MATLAB, as shown in Fig. 5. The results show that the required valve rotation angle is always within the range of -35° to 35° at different walking speeds,

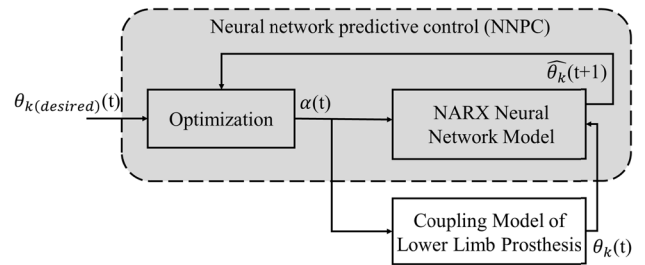


FIGURE 6. Structure block diagram of NNPC.

and it can flexibly provide the required bidirectional damping torque in the swing phase and can switch smoothly between flexion and extension damping without suddenly rotating a large angle to avoid the slow response of the motor, indicating that the valve structure meets the design requirements.

III. NEURAL NETWORK PREDICTIVE CONTROL IN SWING PHASE

Considering that the knee prosthesis is a nonlinear and strongly coupled system, in order to ensure the gait symmetry of the wearers, NNPC is proposed to realize the adaptive damping control of the knee prosthesis. NNPC can predict future variables and adopt corresponding control strategies [24], [25].

A. ALGORITHM OVERALL STRUCTURE

Fig. 6 shows the structure block diagram of NNPC, consisting of the nonlinear auto-regressive with external input (NARX)

$$M_k = \left(\frac{\rho A^3 b^2 s^2 \cos^2(\theta_s - \theta_t) (\dot{\theta}_s - \dot{\theta}_t)}{8C_d^2 \left[\int_r^d [\cos(55^\circ - \alpha) - \sin 35^\circ] \sqrt{\left(\frac{d}{2}\right)^2 - t^2} dt \right]^2 [b^2 + s^2 + 2bs \sin(\theta_s - \theta_t)]} + k \Delta x \right) \cdot \frac{bs \cos(\theta_s - \theta_t)}{\sqrt{b^2 + s^2 + 2bs \sin(\theta_s - \theta_t)}} \quad (15)$$

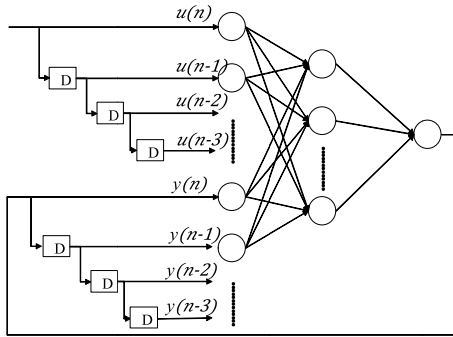


FIGURE 7. Topology of NARX neural network.

neural network model and the optimization block. The aim of the controller is to calculate a suitable valve rotation angle for the hydraulic damper to generate appropriate torque at the knee and enabled the knee prosthesis to accomplish near to healthy swing phase trajectory. The input of NNPC is the desired knee angle ($\theta_k(desired)$) and measured knee angle (θ_k), and the output is the control valve rotation angle (α). To achieve the purpose of predictive control, NNPC needs an algorithm to estimate the future knee angle trajectory when the fan valve rotates at a set angle. Thus, the NARX neural network model is contained in NNPC to complete this task, in which the measured knee angle and the valve rotation angle are input to predict the future knee angle. In each prediction horizon, the optimization block determines the optimal value of the valve rotation angle. Throughout each control interval, the measured knee angle information (θ_k) is fed back to NNPC to achieve closed-loop control [24]. Considering the time delay in the regulation of hydraulic damping, the prediction horizon was determined to be 20 ms after testing the response time of hydraulic damping and motor.

NARX is a dynamic neural network composed of TDL delay layer, input layer, output layer and hidden layer, as shown in Fig. 7 [26]. The signal vector data applied to the multilayer perceptron input layer are as follows: input signal outside the network and its delay: $u(n), u(n-1), \dots, u(n-q+1)$; output signal and its delay: $y(n), y(n-1), \dots, y(n-q+1)$. The dynamic behavior of NARX is described by $y(n+1) = f(y(n), \dots, y(n-q+1), u(n), \dots, u(n-q+1))$, where $f()$ is a nonlinear function of its independent variable [27].

B. NNPC PREDICTION PROCESS

To determine the appropriate valve rotation angle, NNPC has a mechanism to simulate the knee prosthesis movement at any valve rotation angle. It uses the NARX neural network model to get predicted knee angle in each process of iteration optimization to obtain the optimal valve rotation angle. The NNPC prediction principle of the knee joint angle during swing phase is shown in Fig. 8.

The calculation process of the NARX neural network in NNPC is shown in Fig. 9. At time t , the valve rotation angle (α) and the measured knee angle (θ_k) are used as the inputs of

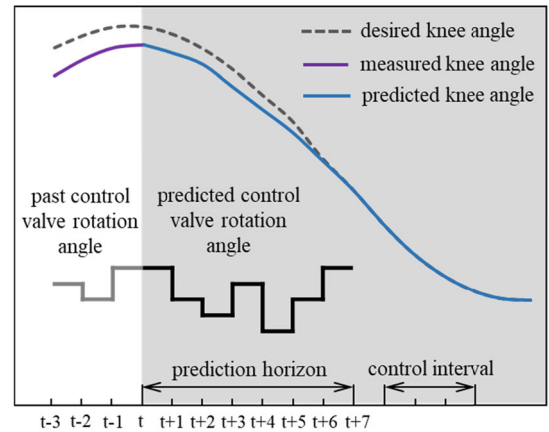


FIGURE 8. NNPC prediction principle of the knee joint angle during swing phase.

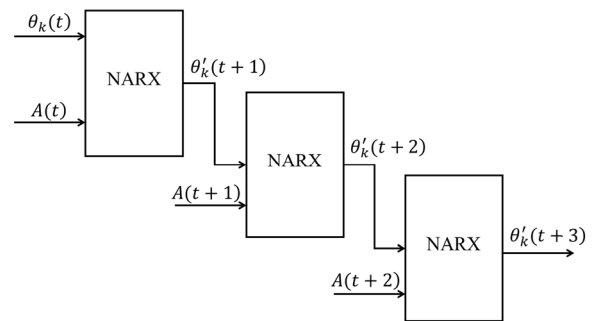


FIGURE 9. Calculation process of NARX neural network.

the NARX neural network model. The model first predicted the knee angle at time $t+1$, and then take the knee angle predicted at time $t+1$ and the random valve rotation angle as the input data of the model, thus predicting the knee angle at time $t+2$.

In Fig. 9, $\theta_k(t)$ is the measured knee angle at time t , $A(t)$ is the random valve rotation angle at time t , and $\theta'_k(t+1)$, $\theta'_k(t+2)$, and $\theta'_k(t+3)$ are the predicted knee angle at time $t+1$, $t+2$, and $t+3$, respectively. The loop proceeds in this way until the maximum prediction horizon is reached. NNPC optimizes these valve rotation angle signals and chooses the one with the least error.

IV. IMPLEMENTATION

A. KNEE PROSTHESIS PROTOTYPE AND GAIT SIMULATION AND EVALUATION WORKBENCH

The prototype of the knee prosthesis uses similar frame to our previous hydraulic knee design [14] to reduce development cost and time, as is shown in Fig. 10. The novel hydraulic microprocessor-controlled damper is installed in the external housing. The top of the piston rod is coaxially connected to the thigh section of the knee prosthesis, and the bottom of the hydraulic cylinder is coaxially connected to the shank section. A DC motor (Maxon Motor DCX10L, 4.5V, 1.5W, gear stage 16:1) acts as the power source for the fan valve rotation.



FIGURE 10. Prototype of the knee prosthesis.

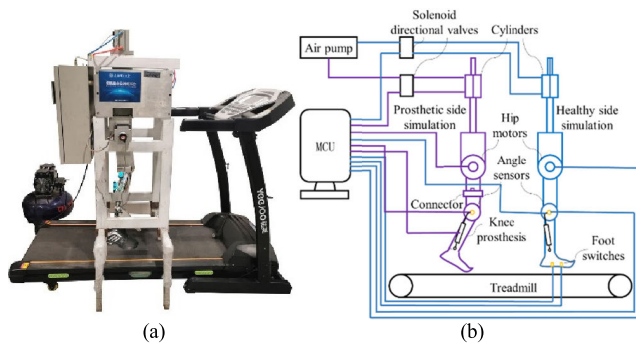


FIGURE 11. The principle and prototype of the workbench. (a) Prototype, (b) Design principle.

A load cell (HBM, JHBM-H3) is installed in the ankle pylon to measure the ground reaction force data. An angle encoder (MIRAN, WOA-C) is installed on the knee rotation axis to measure the knee angle data. A miniature 9-axis inertial sensor (LPMS-ME1, ALUBI) attached to the ankle joint is used to measure the trajectory of the prosthetic limb end.

The total weight of the knee prosthesis is estimated as 1489 g, which includes the hydraulic microprocessor-controlled damper (928 g), the outer structure and tube adapter (445 g), and a battery (116 g), which is lighter than the most similar and advanced commercial variable-damping knee prosthesis, C-Leg 4® (2.47 kg, Otto Bock Healthcare, GmbH, Duderstadt, Germany).

The final knee prosthesis prototype is assembled on a self-built gait simulation and evaluation workbench to implement the proposed control method and quantitatively evaluate overall system performance. The principle and prototype of the workbench are shown in Fig. 11. The mechanical structure of the proposed platform is composed of healthy leg module and prosthetic leg module. The workbench has two main functions: (1) Simulating and measure normal hip and knee angles in real time at different speeds; (2) Simulating the driving force of hip joint on the prosthetic side to evaluate the performance of the knee prosthesis. Angle sensors are used to record the knee angle data of the healthy and prosthetic leg.

TABLE 2. Parameters for NARX.

Parameter	Value
Input delay module	3
Feedback delay module	3
Number of hidden layer neurons	10
Training algorithm	Trainlm (Levenberg-Marquardt)
Error function setting	Mean Squared Error (MSE)

B. ONLINE SIMULATION OF NNPC DURING SWING PHASE

In order to preliminarily verify the control effect of the algorithm at different speeds, the simulation was carried out based on MATLAB platform. The predicted knee angle (θ'_k) and control valve rotation angle (α) during swing phase were simulated and analyzed at slow speed of 0.6m/s, medium speed of 1.1m/s and fast speed of 1.6m/s.

1) SIMULATION SET UP

The simulation system is constructed by MATLAB Simulink and consists of the NNPC controller and the coupling model of workbench, as shown in Fig. 12. In the coupling model of workbench, the hip and knee joints of the healthy side and the hip joint of the prosthetic side are driven by motors according to the desired knee angle data ($\theta_{k(desired)}$) and absolute angle of thigh from the horizontal (θ_t) measured in Section III-C, so as to simulate actual hip or knee trajectories of the subject at different walking speeds. The knee joint of the prosthetic side, the knee prosthesis, is controlled by the NNPC controller, which has a constraint that the knee angle cannot go below 0.

In the NNPC controller, the NARX neural network is used to construct the prediction model, which is set as the parameters in Table 2. The training dataset includes two inputs of knee angle and valve rotation angle, and one output of future knee angle. In order to generate the training dataset, the hip joint on the prosthetic side of the workbench runs according to the set trajectory, the valve rotation angle of the knee prosthesis changes randomly every 20 ms in the range of -35° to 35° . The training dataset including 600 inputs and outputs of NARX model is finally generated. The dataset is randomly divided into three groups, which are composed of training data, validation data and test data in the ratio of 60:20:20.

The Levenberg-Marquardt algorithm [28] is applied for training. The error function is set at the mean square error (MSE). The training process will stop when the MSE value does not significantly decrease within 5 iterations or reach the maximum number of iterations (set to 200). The NARX model and the overall NNPC model are optimized for convergence respectively, and the convergence states are shown in Fig. 13. The mean squared errors of the NARX model and the overall NNPC model reach 10^{-12} and 10^{-6} respectively, reaching the target requirements.

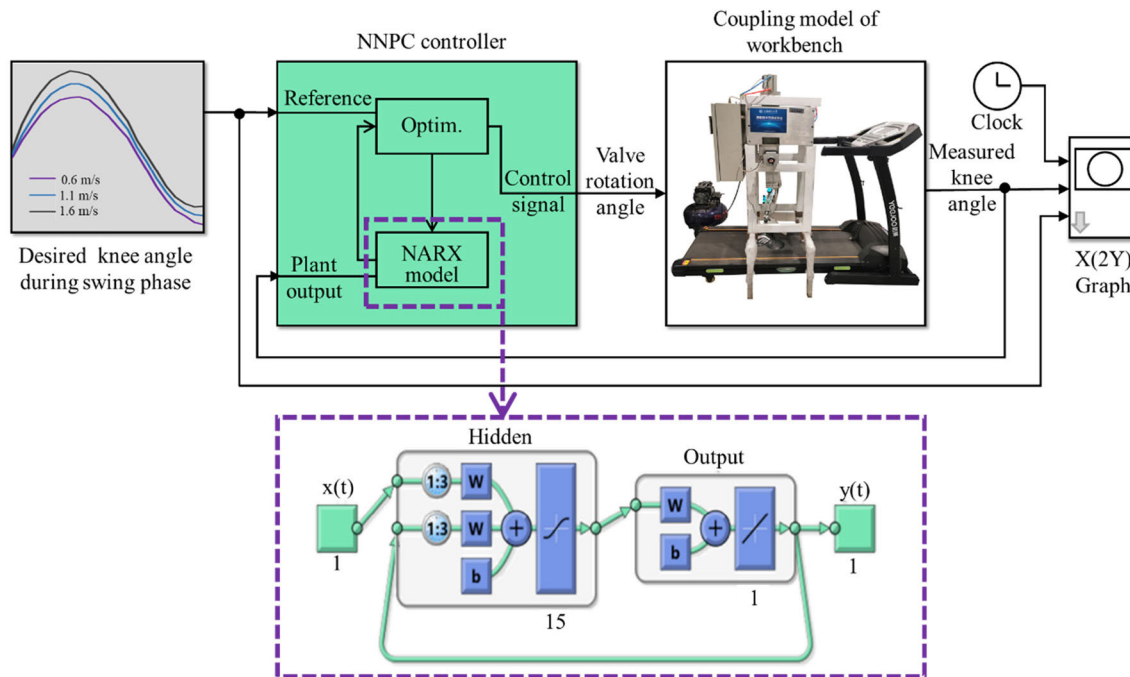


FIGURE 12. NNPC simulation system.

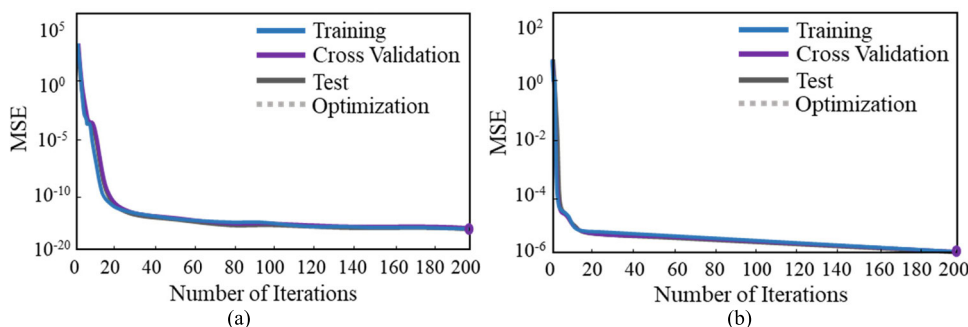


FIGURE 13. Convergence states of models. (a) NARX, (b) NNPC.

2) SIMULATION RESULTS

The results of NNPC during swing phase are shown in Fig. 14. The position in which the two channels are free is set to the initial position of the fan valve, and the counterclockwise rotation is the positive direction of the valve rotation. As shown in Fig. 3, the valve rotation angle is 35° when the flexion channel is blocked, -35° when the extension channel is blocked, and -70° when the two channels are blocked.

Table 3 shows the normalized root mean square errors (NRMSE) of the control model at three different walking speeds. The error results of the controller are collected as the mean value from stable runs out of 50 runs.

From the simulation results, it can be seen that the knee angle obtained by NNPC has a high approximation to the desired healthy knee angle at different speeds, but the error rate of the predictive control model increases as the speed increases.

TABLE 3. NRMSE of NNPC model at three different walking speeds.

Walking Speed [m/s]	NRMSE [%]
0.6	1.04
1.1	1.92
1.6	2.89

V. OFFLINE GAIT SYMMETRY EXPERIMENTS

In order to more intuitively and effectively compare the trajectory tracking performance of NNPC with the fuzzy logical control proposed in the previous work [14], and verify that NNPC can improving the approximation of healthy gait characteristics, a knowledge base containing the mapping relationship between walking speeds and valve rotation angles is established to realize the offline closed-loop control. The diagram of the gait symmetry experiments is shown in Fig. 15.

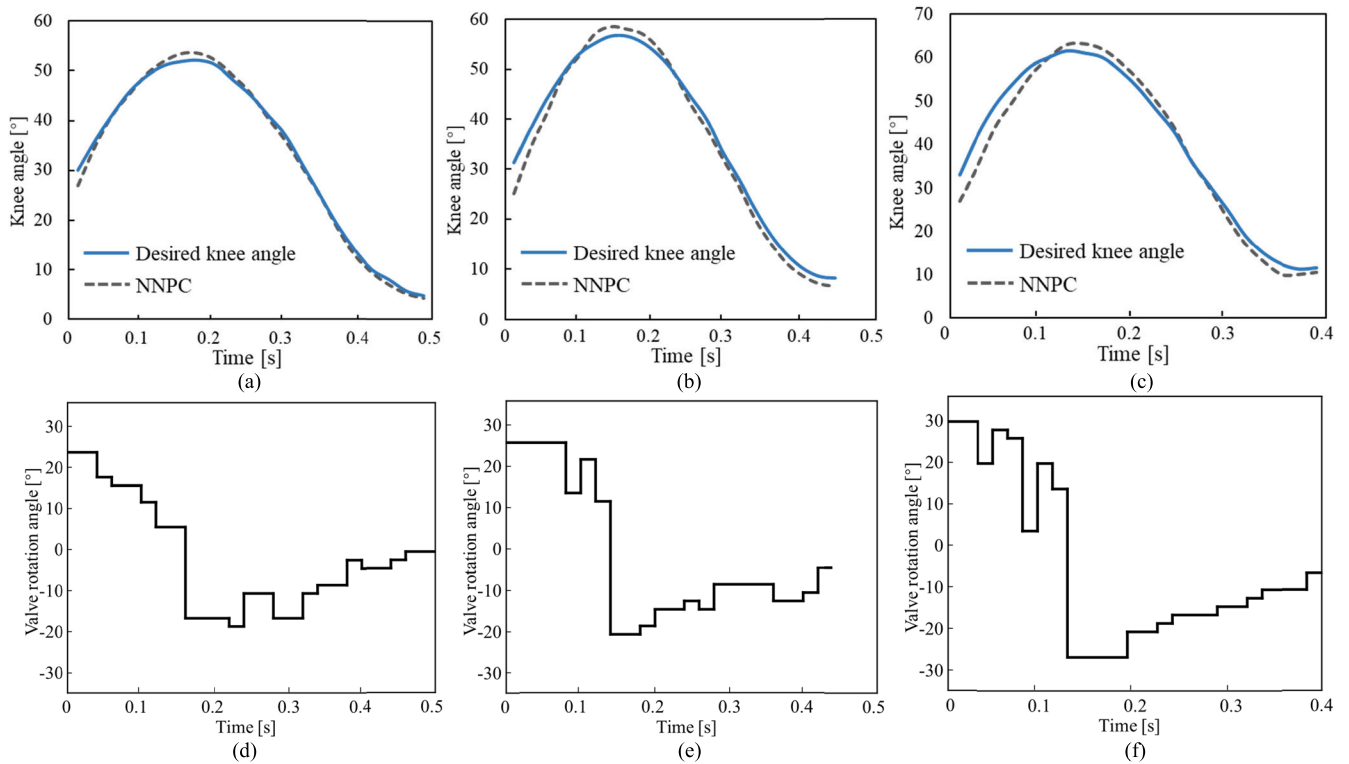


FIGURE 14. Valve rotation angle and knee angle obtained by simulations at three walking speeds during swing phase. (a) Knee angle at 0.6m/s, (b) Knee angle at 1.1m/s, (c) Knee angle at 1.6m/s, (d) Valve rotation angle at 0.6m/s, (e) Valve rotation angle at 1.1m/s, (f) Valve rotation angle at 1.6m/s.

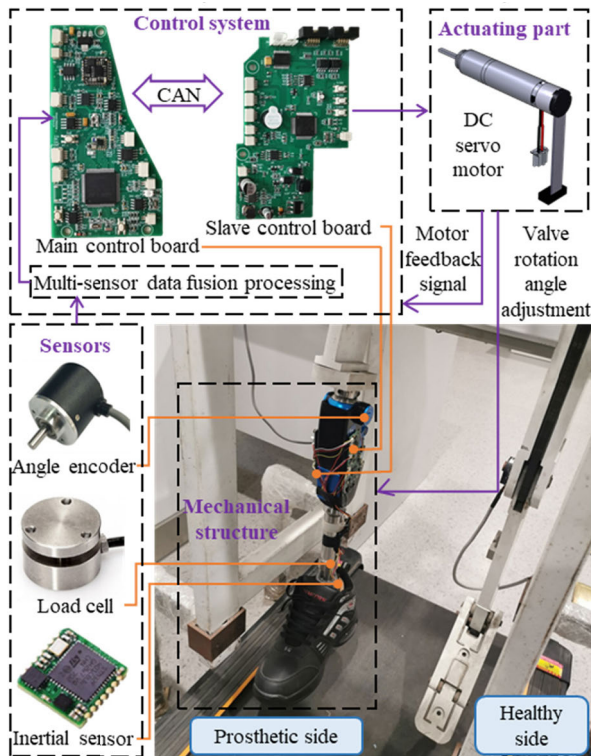


FIGURE 15. The diagram of the gait symmetry experiments.

state when the valve rotates 30 degrees during this phase. The division of stance phase and swinging phase can be realized by the load cell in the ankle pylon. The pressure signal greater than 0 means entering the stance phase, and the pressure signal means entering the swing phase. The force signal greater than 0 means entering the stance phase, and equal to 0 means entering the swing phase. The gait symmetry is the gait parameters which contain the information of gait characteristics selected from the gait cycle to calculate the gait differences between the healthy and prosthetic legs, representing the adaptability to speed changes of the variable-damping knee prosthesis using neural network predictive control [29]. Four indices introduced by Błażkiewicz *et al.* [30] are used to evaluate the gait symmetry. Assuming that $X_L < X_R$, where X_R and X_L are the values of the defined parameter for the healthy and prosthetic limbs.

(1) RI (Ratio Index): $RI = \left(1 - \frac{X_L}{X_R}\right) \cdot 100\%$

RI = 0 indicates complete symmetry, while $RI \geq 100\%$ indicates asymmetry.

(2) SI (Symmetry Index): $SI = \frac{|X_L - X_R|}{0.5 \cdot (X_L + X_R)} \cdot 100\%$

SI = 0 indicates complete symmetry, while $SI \geq 100\%$ indicates asymmetry.

(3) GA (Gait Asymmetry): $GA = \ln\left(\frac{X_R}{X_L}\right) \cdot 100\%$

GA = 0 indicates complete symmetry, while $GA \geq 100\%$ indicates asymmetry.

(4) SA (Symmetry Angle): $SA = \frac{45^\circ - \arctan\left(\frac{X_L}{X_R}\right)}{90^\circ} \cdot 100\%$

SA = 0 indicates complete symmetry, while $SA \geq 100\%$ indicates asymmetry.

Since the major function of the knee prosthesis during stance phase is to support the body weight and ensure stability, the flexion damping is adjusted to the highly damped

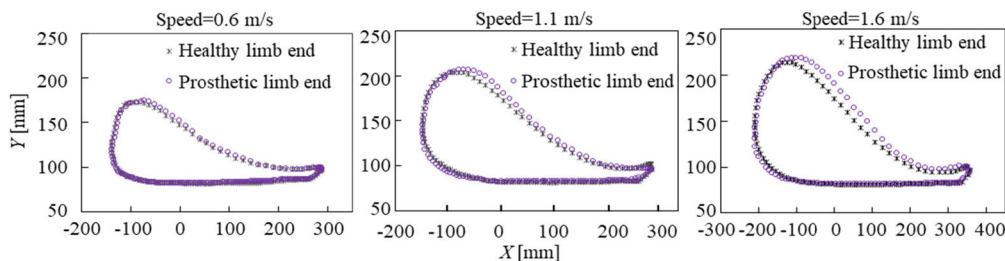


FIGURE 16. The motion curves of the healthy limb end and prosthetic limb end.

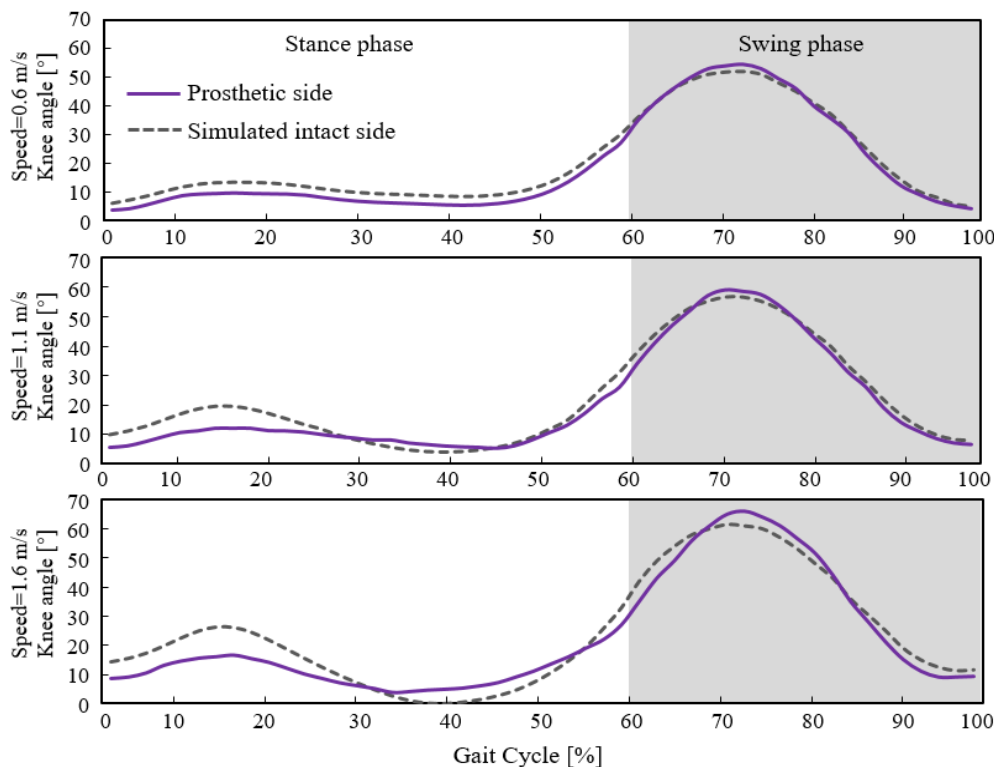


FIGURE 17. The knee angle of the both sides at different walking speeds.

Fifty gait cycles that were effectively divided into stance phase and swing phase by the load cell were selected to evaluate the symmetry indices between healthy and prosthetic angles at different speeds. The angles of healthy and prosthetic knee were transformed in the same gait cycle to show the periodicity. The healthy and prosthetic limb end motion curves and knee angle trajectories at 0.6 m/s, 1.1 m/s and 1.6 m/s, respectively, are shown in Fig. 16 and Fig. 17. Table 4 shows the values of symmetry indices calculated at these three walking speeds. It shows that there is a significant difference in symmetry between stance phase and swing phase and the gait is more asymmetrical during stance phase than during swing phase. This is due to the valve maintains a fixed high flexion damping position during stance phase, which results in the standing flexion angle of the knee joint smaller than the normal value. Since this article mainly studies the control method of swing phase, it focuses on the gait symmetry of swing phase rather than stance phase. During swing phase, the four indices are all smaller than

TABLE 4. Symmetry indices data calculated under different speeds.

Walking Speed [m/s]	Gait Phase	RI [%]	SI [%]	GA [%]	SA [%]
0.6	stance	29.71	35.25	35.70	11.09
	swing	6.35	6.68	6.70	2.12
1.1	stance	27.80	30.65	31.13	9.61
	swing	8.51	9.06	9.42	2.99
1.6	stance	89.06	60.54	78.88	17.62
	swing	11.65	12.08	12.67	3.99

their boundary values at different walking speeds, $RI < 12$, $SI < 13$, $GA < 13$, $SA < 4$. As the speed increases, the value of the indices increase, which is the same as the simulation result based on MATLAB.

VI. DISCUSSION

The variable-damping knee prosthesis with a novel hydraulic damper using the neural network predictive control scheme

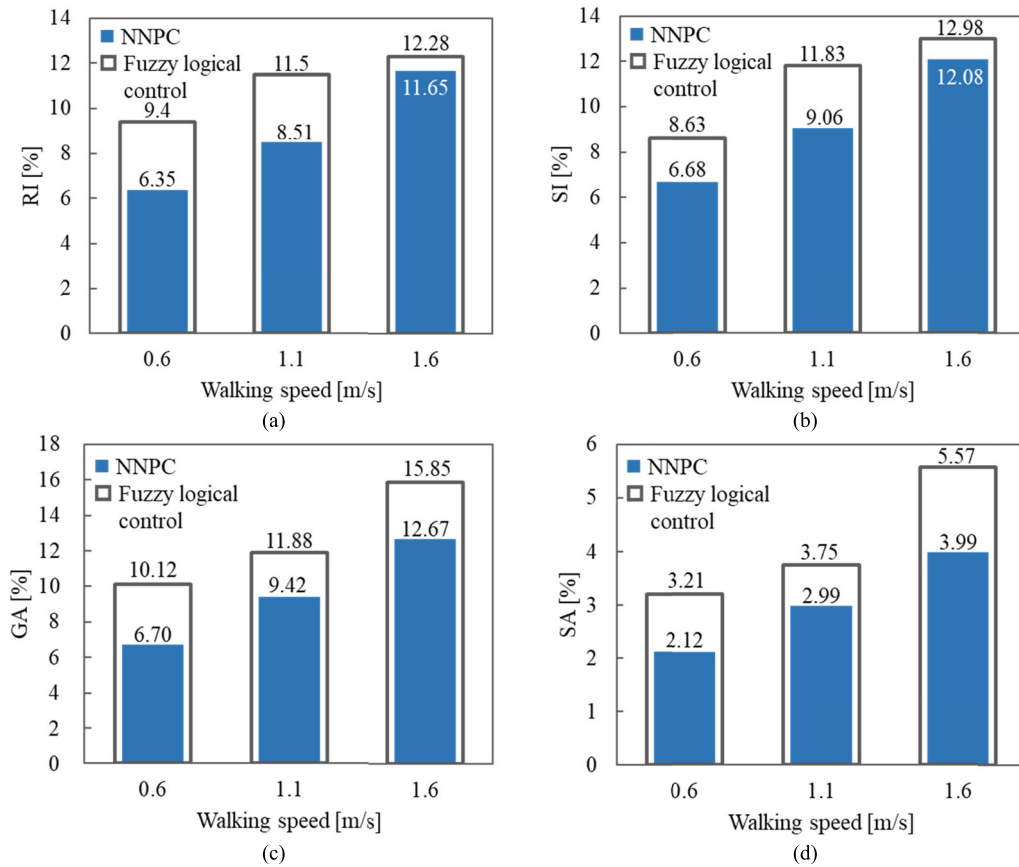


FIGURE 18. Histograms of values of the RI, SI, SA and GA symmetry indices using NNPC and fuzzy logical control. (a) RI values, (b) SI values, (c) GA values, (d) SA values.

during swing phase was proposed in this article. The novel hydraulic damper is provided with an external fan valve structure. In the previous work of our team, two needle valves were respectively controlled by two linear motors [15], in order to fix this shortcoming, we designed a built-in butterfly valve structure controlled by a single motor [14]. However, when the oil is compressed in the chamber, the motor will suffer a great axial load, which will lead to out-of-step and inability to reach the specified position during the adjustment process, seriously affecting the performance of the damping adjustment of the prosthesis. In this article, the external fan valve structure of the hydraulic damper can not only realize independent and continuous adjustment of flexion and extension damping by a single motor, but also can effectively avoid the axial load acting on the motor in the damping cylinder.

NNPC is proposed to use as a controller to control the novel hydraulic damper during swing phase. The simulation was carried out based on MATLAB platform utilizing the coupling model of workbench composed of knee prosthesis prototype and gait simulation and evaluation platform, so as to preliminarily verify the online feasibility and effectiveness of the algorithm at different speeds. In the previous work of our team [14], a fuzzy logical speed adaptive control scheme

based on maximum flexion angle during swing phase was designed to realize the automatic adjustment of damping, but the walking speed need be classified and a knowledge base containing the mapping relationship between the walking speeds and the valve opening need be established. In order to more intuitively and effectively compare the trajectory tracking performance of NNPC with the fuzzy logical control, a knowledge base containing the mapping relationship between walking speeds and valve rotation angles is established according to results of the online simulation of NNPC, and the results of the offline gait symmetry experiments show that symmetry degree is in the normal range. The knee joint trajectories obtained by the similar gait symmetry experiments of fuzzy logical control can be seen in [14], and the calculated indices values of swing phase using the same four indicators as in this article are shown in the Table 5. Fig. 18 shows the comparison of the symmetry indices values between NNPC and fuzzy logical control.

The results indicate that NNPC improves the gait symmetry from the fuzzy logical control at different walking speeds as the values of symmetry indices are significantly decrease in the range of 5.13% to 33.96%. This is because fuzzy logical control can only adjust the valve angle twice when entering the swing flexion and swing extension phase, and cannot

TABLE 5. Symmetry indices data in swing phase using fuzzy logical control.

Walking Speed [m/s]	RI [%]	SI [%]	GA [%]	SA [%]
0.6	9.40	8.63	10.12	3.21
1.1	11.50	11.83	11.88	3.75
1.6	12.28	12.98	15.85	5.57

accurately track the angle trajectory of healthy knee joint, whereas NNPC has the ability to determine a suitable value rotation angle during each control interval, thus providing better gait symmetry.

VII. CONCLUSION

This study proposed a variable-damping knee prosthesis with a novel hydraulic damper using neural network predictive control (NNPC) scheme during swing phase. The external fan valve structure of the hydraulic damper can not only realize independent and continuous adjustment of flexion and extension damping by a single motor, but also can effectively avoid the damping adjustment failure caused by excessive load. NNPC was proposed to use as a controller to control the novel hydraulic damper during swing phase. The simulation was carried out based on MATLAB platform utilizing the coupling model of workbench composed of knee prosthesis prototype and self-built gait simulation and evaluation platform, so as to preliminarily verify the online feasibility and effectiveness of the algorithm at different speeds. In order to more intuitively and effectively compare the trajectory tracking performance of NNPC with the fuzzy logical control proposed in previous work of our team, the offline gait symmetry experiments are designed to observe its performance by evaluating symmetry indices based on the workbench. The values of symmetric indices obtained by the two control methods are compared. These results indicate that NNPC can mimic knee trajectory of a normal gait and generates better results compared to the fuzzy logical control. To sum up, the proposed variable-damping knee prosthesis can make a good performance on improving the approximation of healthy gait characteristics and meet the fundamental requirements of walking at various walking speeds. In the future work, online control and optimization will be realized by running NNPC on microcontrollers.

REFERENCES

- [1] G. Fiedler, J. Akins, R. Cooper, S. Munoz, and R. A. Cooper, "Rehabilitation of people with lower-limb amputations," *Current Phys. Med. Rehabil. Rep.*, vol. 2, no. 4, pp. 263–272, Sep. 2014, doi: [10.1007/s40141-014-0068-8](https://doi.org/10.1007/s40141-014-0068-8).
- [2] S. Sundarapandian, S. Ferris-Francis, H. Michko, C. Charters, J. Miller, and N. Prabakar, "A novel communication architecture and control system for TeleBot: A multi-modal telepresence robot for disabled officers," *Int. J. Next Gener. Comput.*, vol. 7, no. 3, pp. 222–237, Nov. 2016.
- [3] W. Cao, C. Chen, H. Hu, K. Fang, and X. Wu, "Effect of hip assistance modes on metabolic cost of walking with a soft exoskeleton," *IEEE Trans. Autom. Sci. Eng.*, early access, Oct. 23, 2020, doi: [10.1109/TASE.2020.3027748](https://doi.org/10.1109/TASE.2020.3027748).
- [4] K. Ekkachai, A. Tantaworrasilp, S. Nithi-Uthai, K. Tungpimolrut, and I. Nilkhamhang, "Variable walking speed controller of MR damper prosthetic knee using neural network predictive control," in *Proc. SICE Annu. Conf. (SICE)*, Sapporo, Japan, Sep. 2014, pp. 513–518.
- [5] J. L. Johansson, D. M. Sherrill, P. O. Riley, P. Bonato, and H. Herr, "A clinical comparison of variable-damping and mechanically passive prosthetic knee devices," *Amer. J. Phys. Med. Rehabil.*, vol. 84, no. 8, pp. 563–575, Aug. 2005, doi: [10.1097/01.phm.0000174665.74933.0b](https://doi.org/10.1097/01.phm.0000174665.74933.0b).
- [6] W. Cao, W. Zhao, H. Yu, W. Chen, and Q. Meng, "Maximum swing flexion or gait symmetry: A comparative evaluation of control targets on metabolic energy expenditure of amputee using intelligent prosthetic knee," *BioMed Res. Int.*, vol. 2018, pp. 1–8, Nov. 2018, doi: [10.1155/2018/2898546](https://doi.org/10.1155/2018/2898546).
- [7] S. Seid, S. Chandramohan, and S. Sujatha, "Optimal design of an MR damper valve for prosthetic knee application," *J. Mech. Sci. Technol.*, vol. 32, no. 6, pp. 2959–2965, Jun. 2018, doi: [10.1007/s12206-018-0552-7](https://doi.org/10.1007/s12206-018-0552-7).
- [8] X. Bonnet, H. Pillet, P. Fodé, F. Lavaste, and W. Skalli, "Gait analysis of a transfemoral amputee with a hydraulic polycentric knee prosthesis," *Comput. Methods Biomech. Biomed. Eng.*, vol. 12, no. 1, pp. 59–60, Aug. 2009, doi: [10.1080/10255840903065530](https://doi.org/10.1080/10255840903065530).
- [9] H.-J. Ahn, K.-H. Lee, and C.-H. Lee, "Design optimization of a knee joint for an active transfemoral prosthesis for weight reduction," *J. Mech. Sci. Technol.*, vol. 31, no. 12, pp. 5905–5913, Dec. 2017, doi: [10.1007/s12206-017-1134-9](https://doi.org/10.1007/s12206-017-1134-9).
- [10] B. E. Lawson, B. Ruhe, A. Shultz, and M. Goldfarb, "A powered prosthetic intervention for bilateral transfemoral amputees," *IEEE Trans. Biomed. Eng.*, vol. 62, no. 4, pp. 1042–1050, Apr. 2015, doi: [10.1109/TBME.2014.2334616](https://doi.org/10.1109/TBME.2014.2334616).
- [11] C. Ochoa-Diaz, T. S. Rocha, L. de Levy Oliveira, M. G. Paredes, R. Lima, A. P. L. Bo, and G. A. Borges, "An above-knee prosthesis with magnetorheological variable-damping," in *Proc. 5th IEEE RAS/EMBS Int. Conf. Biomed. Robot. Biomechatronics*, Aug. 2014, pp. 108–113.
- [12] J. W. Michael, "Modern prosthetic knee mechanisms," *Clin. Orthopaedics Rel. Res.*, vol. 361, pp. 39–47, Apr. 1999, doi: [10.1097/00003086-199904000-00006](https://doi.org/10.1097/00003086-199904000-00006).
- [13] M. Rupal, A. Vućina, R. Dedić, and H. Đindo, "Overview of the development of hydraulic above knee prosthesis," in *Proc. CMBEBIH*, Singapore, Mar. 2017, pp. 218–222.
- [14] W. Cao, H. Yu, W. Chen, Q. Meng, and C. Chen, "Design and evaluation of a novel microprocessor-controlled prosthetic knee," *IEEE Access*, vol. 7, pp. 178553–178562, Dec. 2019, doi: [10.1109/ACCESS.2019.2957823](https://doi.org/10.1109/ACCESS.2019.2957823).
- [15] W. Cao, H. Yu, W. Zhao, J. Li, and X. Wei, "Target of physiological gait: Realization of speed adaptive control for a prosthetic knee during swing flexion," *Technol. Health Care*, vol. 26, no. 1, pp. 1–12, Sep. 2017, doi: [10.3233/THC-170981](https://doi.org/10.3233/THC-170981).
- [16] S. Preitl, R.-E. Precup, Z. Preitl, S. Vaivoda, S. Kilyeni, and J. K. Tar, "Iterative feedback and learning control. Servo systems applications," *IFAC Proc. Volumes*, vol. 40, no. 8, pp. 16–27, 2007, doi: [10.3182/20070709-3-RO-4910.00004](https://doi.org/10.3182/20070709-3-RO-4910.00004).
- [17] H. Chen and N. Sun, "Nonlinear control of underactuated systems subject to both actuated and unactuated state constraints with experimental verification," *IEEE Trans. Ind. Electron.*, vol. 67, no. 9, pp. 7702–7714, Sep. 2020, doi: [10.1109/TIE.2019.2946541](https://doi.org/10.1109/TIE.2019.2946541).
- [18] S. Seid, S. Sujatha, and S. Chandramohan, "Design of controller for single axis knee using hydraulic damper," in *Proc. 12th IEEE AFRICON*, Addis Ababa, Ethiopia, Sep. 2015, Art. no. 15603421.
- [19] H. Richter, X. Hui, A. van den Bogert, and D. Simon, "Semiactive virtual control of a hydraulic prosthetic knee," in *Proc. IEEE Conf. Control Appl. (CCA)*, Buenos Aires, Argentina, Sep. 2016, Art. no. 16377825.
- [20] M. Lazar and O. Pastravanu, "A neural predictive controller for nonlinear systems," *Math. Comput. Simul.*, vol. 60, no. 3, pp. 315–324, Sep. 2002, doi: [10.1016/S0378-4754\(02\)00023-X](https://doi.org/10.1016/S0378-4754(02)00023-X).
- [21] *Human Dimensions of Chinese Adults*, Standard GB/T 10000, National Standard the People's Republic of China, Standardization Admin. China, Beijing, China, 1988.
- [22] J. Geeroms, L. Flynn, R. Jimenez-Fabian, B. Vanderborcht, and D. Lefebvre, "Design and energetic evaluation of a prosthetic knee joint actuator with a lockable parallel spring," *Bioinspiration Biomimetics*, vol. 12, no. 2, Feb. 2017, Art. no. 026002, doi: [10.1088/1748-3190/aa575c](https://doi.org/10.1088/1748-3190/aa575c).
- [23] Y. Hong-Liu, X. Zhao-Hong, J. Zhuo, and S. Ling, "Dynamics modeling and analysis for hydraulic intelligent prosthetic leg," *JPO J. Prosthetics Orthotics*, vol. 22, no. 3, pp. 177–182, Jul. 2010, doi: [10.1097/JPO.0b013e3181eaf2da](https://doi.org/10.1097/JPO.0b013e3181eaf2da).

- [24] K. Ekkachai and I. Nilkhamhang, "Swing phase control of semi-active prosthetic knee using neural network predictive control with particle swarm optimization," *IEEE Trans. Neural Syst. Rehabil. Eng.*, vol. 24, no. 11, pp. 1169–1178, Nov. 2016, doi: [10.1109/TNSRE.2016.2521686](https://doi.org/10.1109/TNSRE.2016.2521686).
- [25] N. Chaovalit, W. Kongprawechnon, and K. Ekkachai, "On-line neural network predictive control for swing phase control of MR damper prosthetic knee," in *Proc. 56th Annu. Conf. Soc. Instrum. Control Eng. Jpn. (SICE)*, Kanazawa, Japan, Sep. 2017, Art. no. 17363803.
- [26] T. Lin, B. G. Horne, P. Tino, and C. L. Giles, "Learning long-term dependencies in NARX recurrent neural networks," *IEEE Trans. Neural Netw.*, vol. 7, no. 6, pp. 1329–1338, Nov. 1996, doi: [10.1109/72.548162](https://doi.org/10.1109/72.548162).
- [27] J. B. Gomm, J. T. Evans, and D. Williams, "Development and performance of a neural-network predictive controller," *Control Eng. Pract.*, vol. 5, no. 1, pp. 49–59, Jan., 1997, doi: [10.1016/S0967-0661\(96\)00206-7](https://doi.org/10.1016/S0967-0661(96)00206-7).
- [28] J. J. de Rubio, "Stability analysis of the modified Levenberg-Marquardt algorithm for the artificial neural network training," *IEEE Trans. Neural Netw. Learn. Syst.*, pp. 1–15, Aug. 2020, doi: [10.1109/TNNLS.2020.3015200](https://doi.org/10.1109/TNNLS.2020.3015200).
- [29] R. Queen, L. Dickerson, S. Ranganathan, and D. Schmitt, "A novel method for measuring asymmetry in kinematic and kinetic variables: The normalized symmetry index," *J. Biomech.*, vol. 99, Jan. 2020, Art. no. 109531, doi: [10.1016/j.jbiomech.2019.109531](https://doi.org/10.1016/j.jbiomech.2019.109531).
- [30] M. Błażkiewicz, I. Wiszomirska, and A. Wit, "Comparison of four methods of calculating the symmetry of spatial-temporal parameters of gait," *Acta Bioeng. Biomech.*, vol. 16, no. 1, pp. 29–35, Jul. 2014, doi: [10.5277/abb140104](https://doi.org/10.5277/abb140104).



HE LAN (Member, IEEE) received the B.S. degree in biomedical engineering from South-Central Minzu University, China, in 2017, and the M.S. degree in biomedical engineering from the University of Shanghai for Science and Technology, China, in 2020. He is currently a Lecturer with the Quzhou College of Technology, China. His major research interests include human lower limb movement intention recognition and design and optimization of the distributed information fusion algorithms.



ZHANG ZHEWEN (Member, IEEE) received the B.S. degree in mechanical engineering from Nanjing Tech University, China, in 2019. He is currently pursuing the M.S. degree biomedical engineering with the University of Shanghai for Science and Technology, China. His research interests include bionic structure design of knee prosthesis, structural optimization of intelligent hydraulic damper, and fluid dynamics.



CHANGLONG CHEN (Member, IEEE) received the B.S. degree in electromechanical engineering and automation from Binzhou University, China, in 2019. He is currently pursuing the M.S. degree in biomedical engineering with the University of Shanghai for Science and Technology, China. His research interests include compliant control and adaptive impedance control of nonlinear systems.



HONGLIU YU (Member, IEEE) received the B.S. degree in electrical power engineering from the Huazhong University of Science and Technology, China, in 1987, the M.S. degree in mechanical engineering from Zhengzhou University, China, in 1990, and the Ph.D. degree in industry engineering from the University of Shanghai for Science and Technology, China, in 2009.

From 1990 to 1994, he was an Assistant Professor with East China Jiaotong University, China. From 1994 to 2002, he was a Senior Mechanical Engineer and the Manager with Guangdong Jianlibao FTB Packaging Ltd., China. In 2016, he was a Senior Visiting Scholar with the Department of Computer Science, University of Hamburg, Germany. Since 2002, he has been a Professor and the Director with the Medical Instrument and Food Engineering Department, Rehabilitation Engineering and Technology Institute, University of Shanghai for Science and Technology, China. He is the author of five books, more than 130 articles, and more than 100 patents. As the charging person, he founded the first education program of rehabilitation engineering and technology in China. His research interests include human bionic mechanics and intelligent control, rehabilitation robotics, man-machine intelligent interaction, and orthopedic devices and biomechanics.



XIAOMING WANG (Member, IEEE) received the B.S. degree in biomedical engineering from the University of Shanghai for Science and Technology, China, in 2018, where she is currently pursuing the Ph.D. degree, taking a successive postgraduate and doctoral program. Her research interests include the development of intelligent perception and control of knee prosthesis, man-machine coupled biomechanics and dynamics modeling, and bionic structure design of knee prosthesis.



QIAOLING MENG (Member, IEEE) received the B.S. degree in mechanical engineering from the Shenyang University of Technology, China, in 2002, the M.S. degree from Northeastern University, China, in 2008, and the Ph.D. degree from the University of Bologna, Italy, in 2012.

From 2012 to 2013, she held the postdoctoral position with the University of Macau, Macau. Since 2013, she was an Assistant Professor with the University of Shanghai for Science and Technology, China, where she is currently an Associate Professor. Her current research interests include mechanical bionics, human biomechanics, and robot dynamics.